www.cafetinnova.org

Indexed in
Scopus Compendex and Geobase Elsevier, Chemical Abstract Services-USA, Geo-Ref Information Services-USA, List B of Scientific Journals, Poland, Directory of Research Journals

International Journal of Earth Sciences and Engineering

April 2015, P.P.248-255

ISSN 0974-5904, Volume 08, No. 02

Generation of Site Specific Response Spectrum near Nuclear Power Plants: A Preliminary Case Study at Rawatbhata Station

ABHIJIT MOLAWADE[1], CHENNA RAJARAM[2], RAMANCHARLA PRADEEP KUMAR[2] AND T VIJAY KUMAR[1]

[1]*School of Earth Sciences, Swami Ramanand Teerth Marathwada University Nanded, INDIA*
[2]*Earthquake Engineering Research Centre, IIIT Hyderabad, INDIA*
Email: *molawadeap@gmail.com, rajaram.chenna@research.iiit.ac.in, ramancharla@iiit.ac.in, vijay.srtmu@gmail.com*

Abstract: Nuclear power plant is one of the largest source of producing electricity in India after thermal, hydro-electric and renewable sources of electricity. As of 2013, India has 21 nuclear reactors in operation in 6 nuclear power plants, having an installed capacity of 5780 MW and producing a total of 30, 293 GWh of electricity while six other reactors are under construction and are expected to generate an additional 6,100 MW. After 2011 Fukushima earthquake in Japan, safety of nuclear reactors has become a major concern. For assessing safety it is utmost important to have information on expected earthquake events. In case of lack of sufficient information, artificial ground motions may be generated by using geological features and faults information. This study presents simulation of near field generated ground motions of Rawatbhata nuclear power plant. For this purpose, three faults nearer to the power plant have been selected to the generate ground motions using semi-empirical approach. It is observed that as the source (M) of the earthquake increases, the amplitude of the ground motion, duration and energy content increases. Similarly, the spectral accelerations also increase due to all three active faults.

1. Introduction

Nuclear power is the fourth-largest source of electricity in India after thermal, hydro and renewable sources of electricity. As of 2013, India has 20 nuclear power plants in operation generating 4,780 MW while 6 other are under construction and are expected to generate an additional 2,720 MW (International Atomic Energy Agency; World Nuclear Association). India's nuclear power industry is undergoing rapid expansion with plans to increase nuclear power output to 64G MW by 2032 (Nuclear Power Corporation of India Limited). The country is involved in the development of nuclear fusion reactors through its participation in the International Thermonuclear Experimental Reactor (ITER) project and is a global leader in the development of Thorium based fast breeder reactors (Malhotra S K., 2010).

India's domestic Uranium reserves are small and the country is dependent on Uranium imports to fuel its nuclear power industry. Since early 1990s, Russia has been a major supplier of nuclear fuel to India. Due to dwindling domestic Uranium reserves, electricity generation from nuclear power in India has declined by 12.83% from 2006 to 2008. Following a waiver from the Nuclear Suppliers Group in September 2008 which allowed it to commence international nuclear trade, India has signed bilateral deals on civilian nuclear energy technology cooperation with several other countries including France, United States, United Kingdom, Canada. India has also Uranium supply agreements with Russia, Mangolia, Argentina and Namibia. An Indian private company won a Uranium exploration contract in Nigar.

Nuclear establishment in India is known for its secrecy and the public, by and large, knows little about how the functioning of nuclear activities. In absence of an independent safety regulation body, people fear the safety standards are actually not very high in India. India faces few nuclear accidents in 1991, 1992, 1993, 1994, 1999, 2002, 2003, 2009 and 2010 (Sumanth et al., 2011).

1.1. Seismic safety of NPP

Seismic safety is one of the most important external events of natural origin to be considered for safe design of a Nuclear Power Plant (NPP). Since detailed evaluation of a site is an elaborate process that require great amount of efforts and time, some simple acceptance/rejection criteria have been developed (Bishnoi L.B., 2014). These criteria are applied initially during preliminary site selection process before embarking on detailed evaluation.

First step is to evaluate seismic hazards associated with the NPP site. If the evaluation shows that there are no

#SPL02080243 Copyright ©2015 CAFET-INNOVA TECHNICAL SOCIETY. All rights reserved.

engineering solutions available to protect against or mitigate potential seismic hazards, the site is deemed unsuitable. For acceptable sites, evaluation is carried out in the second step to define earthquake induced design basis ground motion (DBGM) parameters (AERB, 1990b; IAEA, 2002) against which the plant should be engineered. The next step involves seismic response analysis and design of SSC to withstand loading effects of DBGM. Last step is related to operating phase of the plant and it involves monitoring of occurrence of earthquakes and plant response by suitable seismic instrumentation for the purpose of initiation of appropriate protection/mitigation action during or after a seismic event. In this study, Rawatbhata nuclear power plant station has been chosen for generating site specific response spectra. The description of the study has been given in the following sections.

2. Study Area

Strong ground motion plays an important role in safe engineering design of big and important structures. If the site of construction contains no past strong motion records than it poses a major constraint in arriving at earthquake-resistant design parameters. Simulated strong motion records at such sites serve useful purpose for deciding safe design criteria.

Rawatbhata nuclear power plant has been chosen to generate site specific response spectra. The NPP located at 24°52′20″N 75°36′50″E and is about 65 km from Kota by way of the Chambal River. The power plant was constructed in 1963 and operated by Nuclear Power Corporation of India LTD. The first reactor Douglas Point in Canada was begun in 1961, it's duplicate station at Rajasthan, was committed in 1963 (Nuclear Power Corporation of India).

The Rajasthan Atomic Power Plant RAPP included two 220 MWe Canada Deuterium Uranium (CANDU) reactors built in the state of Rajasthan and put into service in 1973 and 1981, respectively. Indian trade's men and professional engineers were trained at Douglas Point. After the nuclear bomb test explosion in 1973 the nuclear trade links between Canada and India were curtailed and the second RAPP reactor was completed by the Indians with no Canadian assistance (Nuclear Power Corporation of India Limited).

After many incidents and repairs Rajasthan Atomic Power Station (RAPS) RAPS-1 has now a 100 MW capacity, RAPS-2 at 200 MW. In the context of the Indian atomic program, two more PHWR with an output of 220 MW each were built. RAPS-3 became critical on 24 December 1999, RAPS-4 became critical on 3 November 2000. Commercial operations began on 1 June 2000 for unit 3, and on 23 December 2000 for unit 4. Two more reactors (RAPS-5 and RAPS-6) with 220 MWe have also been built, with unit 5 beginning commercial operation on 4 February 2010, and unit 6 on 31 March 2010 (Nuclear Power Corporation of India Limited).

The seismicity of India and location of NPP is shown in figure 1 and 2. A MATLAB code is written to generate the ground motions near Rawatbhata NPP (Rajaram and Pradeep, 2014). For this purpose, seismicity around 300 km as radius from the NPP is considered. Three active faults namely FID-663, FID-275 & FID-852 have been chosen in the radius of 45 km and seismicity is considered in the region and the lengths of those faults are 40 km, 36 km and 42 km respectively. It is observed that the minimum and maximum magnitude of earthquakes occurred in the studied region are 4.5 (1866) and 7.2 (1923) respectively (GSI, 2000). Current study shows the variation of ground motion records with respect to magnitude of the earthquake ranges 4.5-7.2. Also response spectra are plotted from the ground motion records.

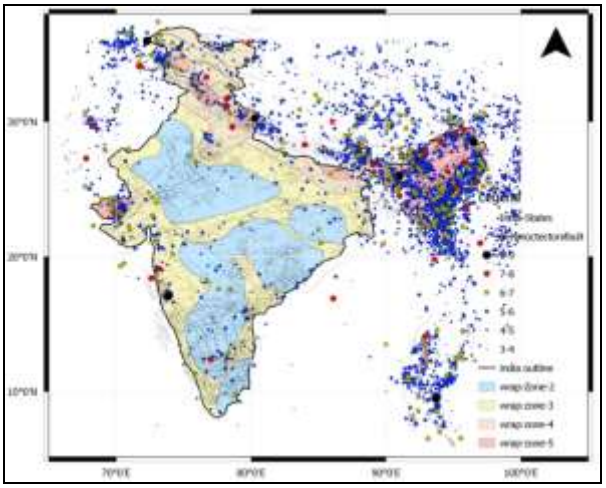

Figure 1 *Seismicity of India since 1898*

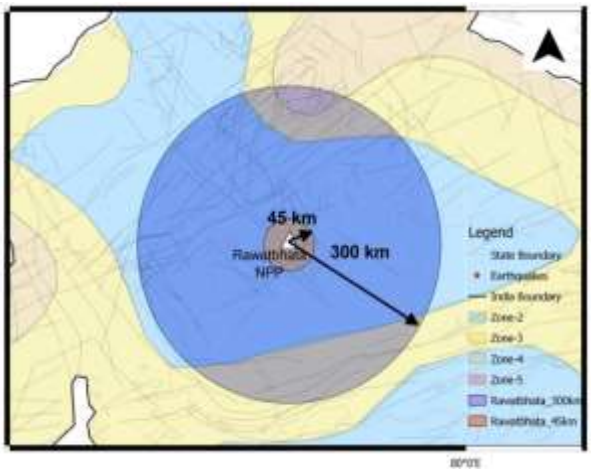

Figure 2 *Location of Rawatbhata NPP in India*

3. Methodology

The technique of semi-empirical simulation is given by Midorikawa (1993) and is based on Ω^2 source model. This technique is modified by Joshi (2004), Joshi and Midorikawa (2004), and Joshi and Mohan (2008) to include the concept of stochastic simulation technique for simulation of strong motion time series. In the first part of this technique, a time series having basic spectral shape of accelerogram is simulated, while in the second part, deterministic model of rupture source has been used to simulate the envelope of accelerogram. The modified semi-empirical method uses the time series obtained from stochastic simulation technique and envelope function obtained from the semi-empirical approach. In the stochastic simulation technique, the white Gaussian noise of zero expected mean and variance chosen to give unit spectral amplitude has been passed through number of filters representing the earthquake processes. In this technique, the amplitude spectrum of white noise is replaced by the acceleration spectra of target earthquake. The shape of acceleration spectra $A(f)$ at a site located at anhypocentral distance R is given as (Boore1983):

$$A(f) = CS(f)\,D_S(f)\,F_R(f,R) \quad (1)$$

Where C is constant scaling factor given by:

$$C = M_0 \cdot R_{\theta\varphi} \cdot FS \cdot PRITITN / 4\pi\rho\beta^3 \quad (2)$$

In this expression, M_0 is the seismic moment, $R_{\theta\varphi}$is the radiation pattern, FS is the amplification due to the free surface, $PRITITN$ is the reduction factor that accounts for the partitioning of total shear wave energy into two horizontal components (taken as $1/\sqrt{2}$), ρ and $\beta$are the density and shear velocity, respectively. The radiation pattern $R_{\theta\varphi}$ is dependent on the type of faulting mechanism and the geometry of earthquake source. The filter $S(f)$ in Eq. (1) is the source acceleration spectrum which is defined by Brune (1970) as follows:

$$S(f) = (2\pi f)^2/[1 + (f/f_c)^2] \quad (3)$$

Filter $D_S(f)$ is the near-site attenuation of high frequencies and is defined as (Boore 1983):

$$D_S(f) = 1/[1 + (f/f_m)^8]^{1/2} \quad (4)$$

The parameter f_m represents the high frequency cutoff range of the high-cut filter. The filter $F_R(f,R)$ represents the effect of anelastic attenuation and is given as (Boore 1983):

$$F_R(f,R) = \left(e^{-\pi f R/\beta Q_\beta(f)}\right)/R \quad (5)$$

Where R denotes the hypocentral distance in km and $Q_\beta(f)$ is the quality factor which defines the frequency-dependent attenuation during the wave propagation. In the present work, the frequency-dependent quality factor $Q_\beta(f)$ for Rawatbhata region is used as $Q_\beta(f) = 167 f^{0.47}$ (Nath and Thingbaijam2009).

The spectrum of white noise after multiplication with theoretical filters given in Eq. (1) represents basic shape of acceleration spectra. Time domain representation of this acceleration spectrum gives an acceleration record that has basic properties of acceleration spectra. However, this time domain representation of acceleration record raises serious problem, like the obtained records overestimate the high frequency strong ground motion and underestimate low frequency in the synthetic strong ground motion. This is due to the difference in duration of slip of the target and the small earthquake considered as sub-faults.

The difference in the duration of slip of the target and the sub-fault earthquake following correction function $F(t)$ given by Irikura et al. (1997) and Irikura and Kamae (1994) is corrected by convolving with the obtained acceleration records:

$$F(t) = \delta(t) + [(N-1)/T_R(1 - \exp(-1))] \cdot \exp(-t/T_R) \quad (6)$$

Where $\delta(t)$ is the delta function, $N$is the total number of sub-faults along the length or the width of the rupture plane, and $T_R$is the rise time of the target earthquake. The convolution of $F(t)$ with obtained acceleration record $a_{ij}(t)$ gives acceleration record $A_{ij}(t)$as:

$$A_{ij}(t) = F(t) * a_{ij}(t) \quad (7)$$

Where i and j represent the position of sub-fault along the length and the width of the rupture plane, respectively. It is observed that stochastic simulation technique requires proper windowing of the obtained record by a function which is based on kinematic representation of model of rupture (Boore 1983). Such time window can be obtained by the semi-empirical technique of Midorikawa (1993) in the form of resultant envelope of accelerogram obtained from a model of finite rupture plane. The finite fault in the semi-empirical technique proposed by Midorikawa (1993) is divided into several sub-faults is based on self-similarity laws proposed by Kanamori and Anderson (1975). Energy is released in the form of acceleration envelop whenever rupture approaches center of elements. The acceleration envelope waveform $e_{ij}(t)$ is determined from the following functional form given by Kameda and Sugito (1978) and further modified by Joshi (2004):

$$e_{ij}(t) = T_{ss}(t/T_d) \cdot \exp(1 - t/T_d) \quad (8)$$

In this expression, $T_d$represents duration parameter and T_{ss}represents the transmission coefficient of incident shear waves. This coefficient is given by the following formula after Lay and Wallace (1995, p. 102) and is

used by Joshi et al. (2001) for modeling the effect of the transmission of energy in the shape of acceleration envelope as:

$$T_{ss} = 2\mu_2\eta_{\beta_2}/(\mu_1\eta_{\beta_1} + \mu_2\eta_{\beta_2}) \quad (9)$$

Where μ_1 and μ_2 are modulus of rigidity in the first and second layers, respectively, and β_1 and β_2 are shear wave velocities in the first and second layers, respectively. The transmission coefficient contributes significantly to shaping the attenuation rate of the peak ground acceleration with respect to the distance from the source. Joshi and Midorikawa (2004) have observed that for the shallow focus earthquakes, the transmission coefficient is not equal to 1.0; however, for the intermediate to deep focus earthquake, this coefficient is approximately equal to 1.0. This means that we should take this coefficient into consideration when modeling an intermediate to deep focus earthquake.

The parameters required to define the model of the rupture plane are its length (L), width (W), length and width of the sub-faults (L_e, W_e), nucleation point, strike and dip of rupture plane (φ_s, δ), rupture velocity (V_r) and shear wave velocity in the medium. The rectangular rupture plane of a target earthquake of seismic moment M_0 is divided into $N \times N$ sub faults of seismic moment M_0': Once the rupture plane of target earthquake is divided into sub-faults, one sub-fault is fixed as nucleation point from which the rupture initiates. This point can coincide with the focus of the earthquake. The rupture starts from the nucleation point and propagates radially within the rupture plane. The sub-fault releases energy whenever the rupture front touches its center. The energy is released in the form of acceleration record $ac_{ij}(t)$, which is the product of acceleration record from stochastic technique with envelope function from semi-empirical simulation technique as:

$$ac_{ij}(t) = e_{ij}(t) \cdot A_{ij}(t) \quad (10)$$

The acceleration record $ac_{ij}(t)$, released from different sub-faults reaches the observation point at different time. The arrival time at the observation point t_{ij} depends on the time taken by rupture from nucleation point to ij^{th} sub-fault with rupture velocity V_r and time taken by energy released from $ijth$ sub-fault to reach the observation point with velocity V of propagation. The total time taken t_{ij} is given as (Joshi and Midorikawa 2004):

$$t_{ij} = \eta_{ij}/V + \xi_{ij}/V_r \quad (11)$$

Where η_{ij} is the distance from the observation point to the ij^{th} sub-fault and ξ_{ij} is the distance travelled by the rupture from nucleation point to particular sub-fault.

In the present work, simple vector notation has been used to resolve these resultant components into horizontal components. The direction of resultant component from each sub-fault is defined by a line joining center of sub-fault to the recording station. This direction is different for different sub-faults and for obtaining horizontal component along strike and perpendicular direction of the modeled rupture plane, records from each sub-fault need separate treatment.

Figure 3 shows the division of total acceleration record $ac_{ij}(t)$ into components along strike and dip directions. Following formula is used for obtaining horizontal component of records along the direction of strike and the direction of dip of the modeled fault, respectively, from resultant component $ac_{ij}(t)$ released by ij^{th} sub-fault. $ac_{ij}^{X}(t)$ and $ac_{ij}^{Y}(t)$ are the acceleration record along X and Y $axis$, respectively, and are defined as follows:

$$ac_{ij}^{X}(t) = ac_{ij}(t) \cdot \cos\theta_{ij} \cdot \cos\varphi_{ij} \quad (12)$$

$$ac_{ij}^{Y}(t) = ac_{ij}(t) \cdot \cos\theta_{ij} \cdot \cos\varphi_{ij} \quad (13)$$

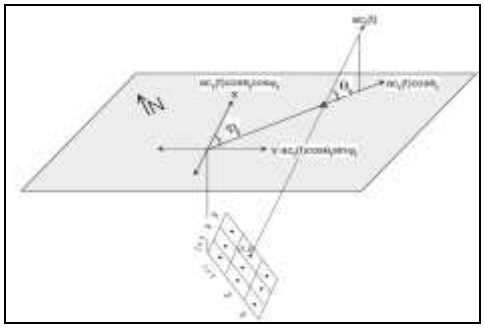

Fig. 3 *Illustration of method for simulation of NS and EW component of earthquake ground motion from ij^{th} sub-fault. Triangle shows the recording station*

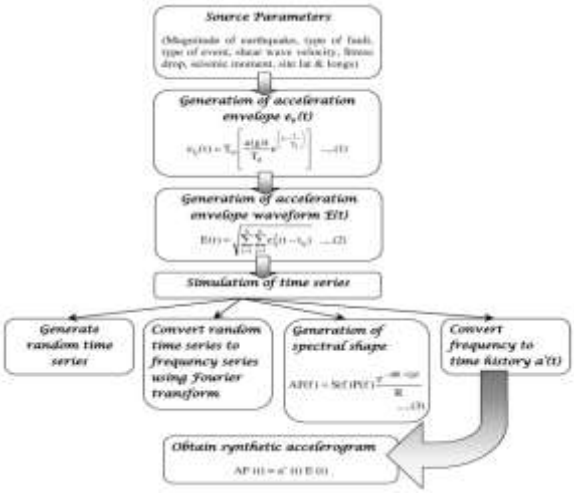

Fig. 4 *flowchart of generation of synthetic accelerogram*

The flowchart of generation of synthetic accelerogram is shown in figure 4. In Eqs. (12) and (13), φ_{ij} represents the angle made by horizontal projection of resultant ground acceleration from ij^{th} sub-fault with the direction of strike of the modeled fault, and θ_{ij} represents the angle made by resultant ground acceleration with the vertical. The angles θ_{ij} and φ_{ij} are different for different sub-faults and depend on the position of sub-fault within the rupture plane. Once the components of acceleration records are obtained along $X-$ and $Y-axis$ for ground acceleration released from a particular sub-fault, it is further rotated by angle $\emptyset$ using following matrix rotation formula to obtain component along $NS$and EW direction.

$$\begin{bmatrix} ac_{ij}^{NS} \\ ac_{ij}^{EW} \end{bmatrix} = \begin{bmatrix} \cos\emptyset & -\sin\emptyset \\ \sin\emptyset & \cos\emptyset \end{bmatrix} \begin{bmatrix} ac_{ij}^{X}(t) \\ ac_{ij}^{Y}(t) \end{bmatrix} \quad (4)$$

Where ac_{ij}^{NS} and ac_{ij}^{EW} are the components of acceleration record along NS and EW direction, respectively, and $\emptyset$ is the strike of the modeled rupture plane measured with respect to the geographic north. Summation of all NS and EW component of acceleration record released from different sub-faults reaching the observation point at different time lag t_{ij} gives the final NS and EW component of acceleration record as follows:

3.1. Characteristics of Ground Motion

For engineering purposes, (1) amplitude (2) frequency and (3) duration of the motion are the important characteristics (Steven L Kramer, 1996). Horizontal accelerations have commonly been used to describe the ground motions. The peak horizontal acceleration (PHA) for a given component of motion is simply the largest (absolute) value of horizontal acceleration obtained from the accelerogram of that component. The largest dynamic forces induced in a certain types of structures (very stiff) are closely related to the PHA.

Earthquakes produce complicated loading with components of motion that span a broad range of frequencies. The frequency content describes how the amplitude of ground motion is distributed among different frequencies. The frequency content of an earthquake motion will strongly influence the motion of structure. The broad band width of the Fourier amplitude spectrum is the range of frequencies over which some level of Fourier amplitude is exceeded. Generally band width is measured at a level of $1/\sqrt{2}$ times of maximum Fourier amplitude. The Fourier transform of an accelerogram $\ddot{x}(t)$ is given by,

$$X(\omega) = \frac{1}{2\pi}\int_{\infty}^{-\infty} \ddot{x}(t)\, e^{-i\omega t} dt \quad (15)$$

Where, $\ddot{x}(t)$is the accelerogram record.

The duration of strong ground motion can have a strong influence on earthquake damage. It is related to the time required for accumulation of strain energy by rupture along the fault. There are different procedures for calculating the duration of ground motion,

Brackted Duration: It is the time between the first and last exceedances of threshold acceleration (usually 0.05 g) (Kramer, 2006)

Trifunac and Brady Duration: It is the time interval between the points at which 5% and 95% of the total energy has been recorded (Kramer, 2006).

3.2. Synthetic Ground Motions

The synthetic ground motions are generated at Rawatbhata NPP due to three active faults with varying magnitude of the earthquake. Results of the same are shown in figure 4, 5 and 6. From the results, it is observed that the fault FID-275 gives higher values of peak ground accelerations. This fault may produce high amount of accelerations in future too. Also, it is observed that as the magnitude of the earthquake increases, the energy content and peak ground acceleration increases. The effect of the source on the ground motion can be clearly seen from figure 4, 5 and 6. The path and site are constant for this case study. As the source of the earthquake reaches to 7.0, the variations in amplitude of the ground motion and duration of the ground motion are increased rapidly. The response spectra are generated for the synthetic ground motions.

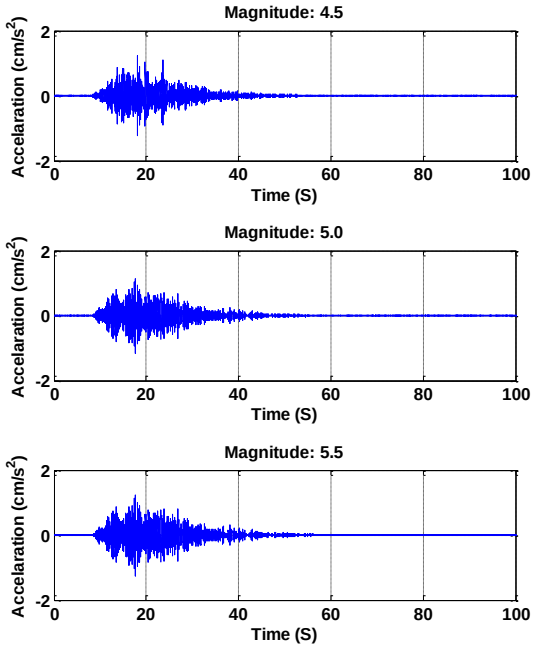

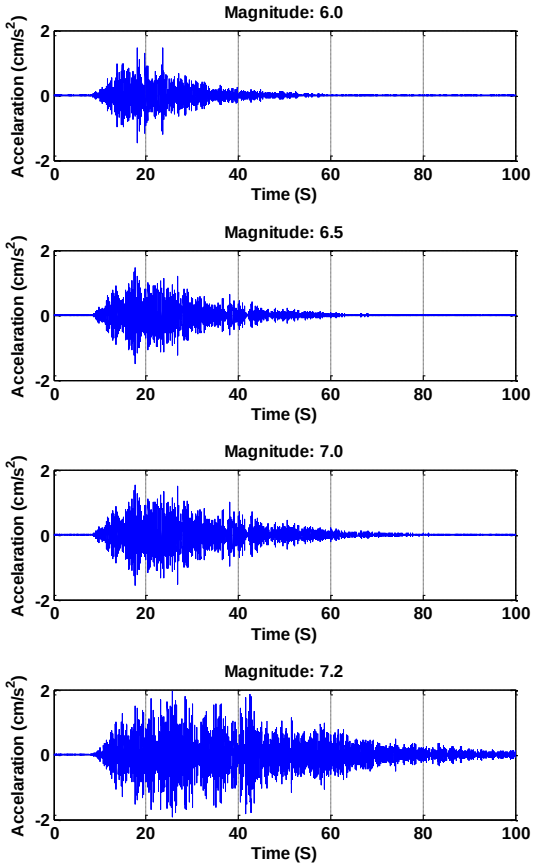

Fig 4 *Synthetic accelerograms with respect to magnitude of the earthquake due to fault FID-663*

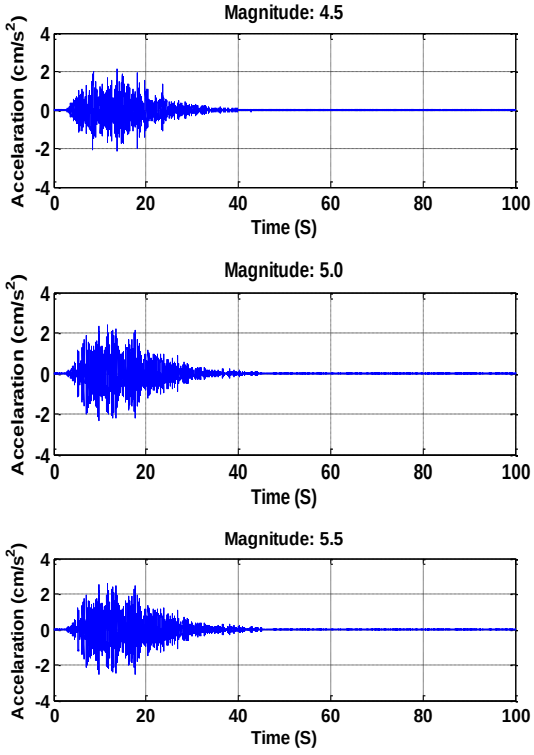

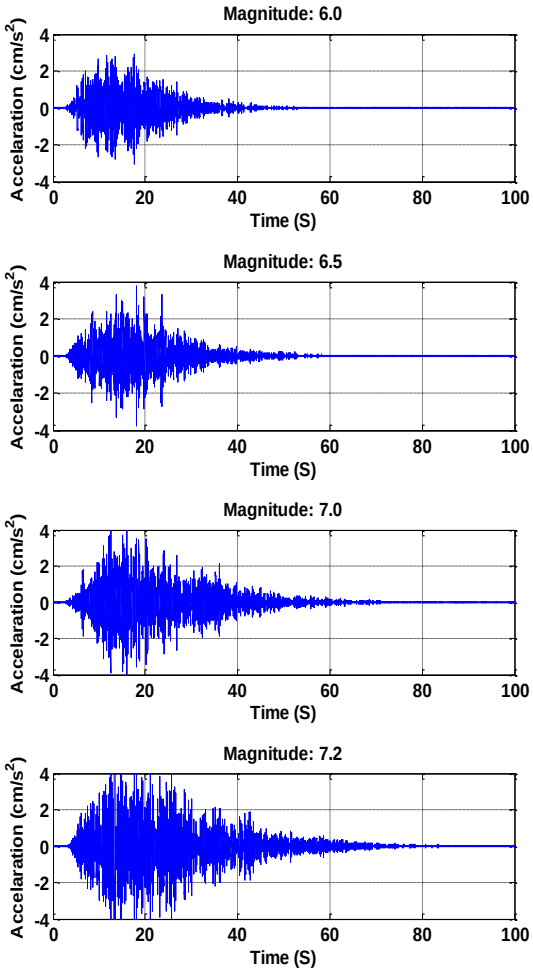

Fig 5 *Synthetic accelerograms with respect to magnitude of the earthquake due to fault FID-275*

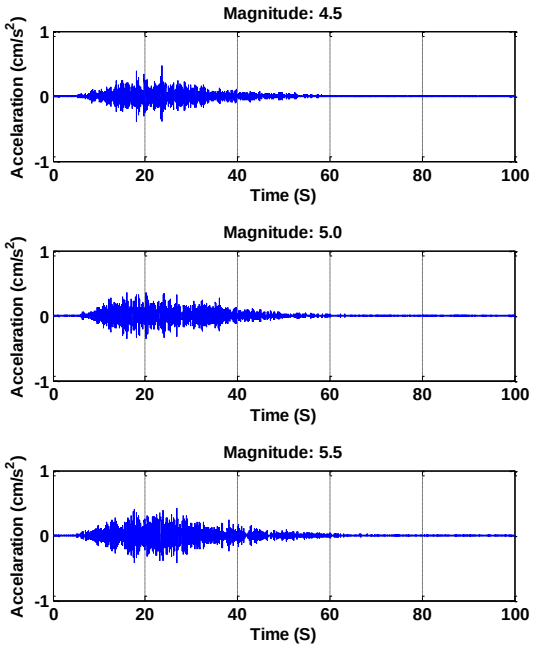

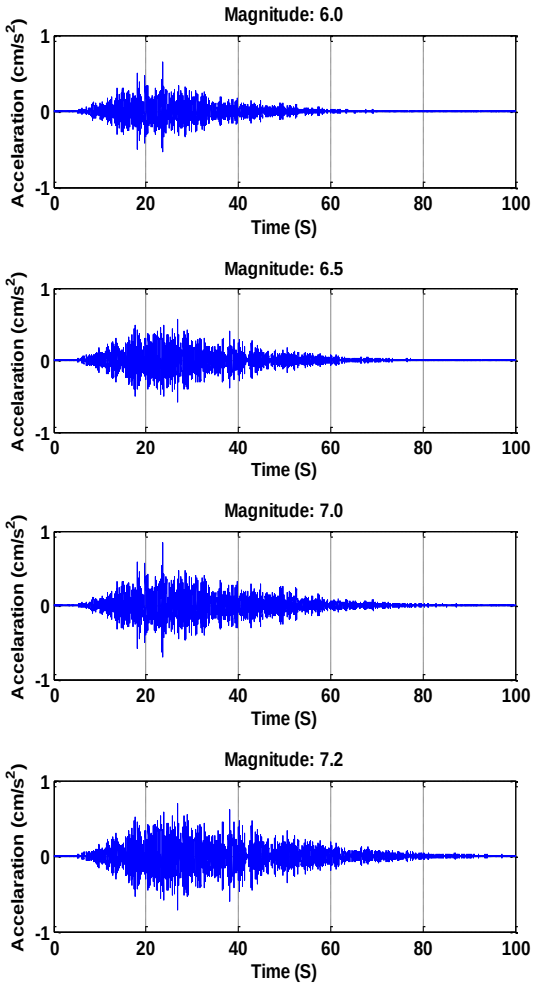

Fig 6 *Synthetic accelerograms with respect to magnitude of the earthquake due to fault FID-852*

3.3. Response Spectra

A response spectrum is simply a plot of the peak responses like displacement, velocity or acceleration of a series of oscillators with varying natural frequency, that are forced into motion by the same base excitation. The resulting plot can then be used to assess the response of building. Response spectra can also be used in assessing the response of linear systems with multiple modes of oscillation (multi-degree of freedom systems), although they are only accurate for low levels of damping. Modal analysis is performed to identify the modes, and the response in that mode can be picked from the response spectrum. This peak response is then combined to estimate a total response. A typical combination method is the square root of the sum of the squares (SRSS) if the modal frequencies are not close. The result is typically different from that which would be calculated directly from an input, since phase information is lost in the process of generating the response spectrum.

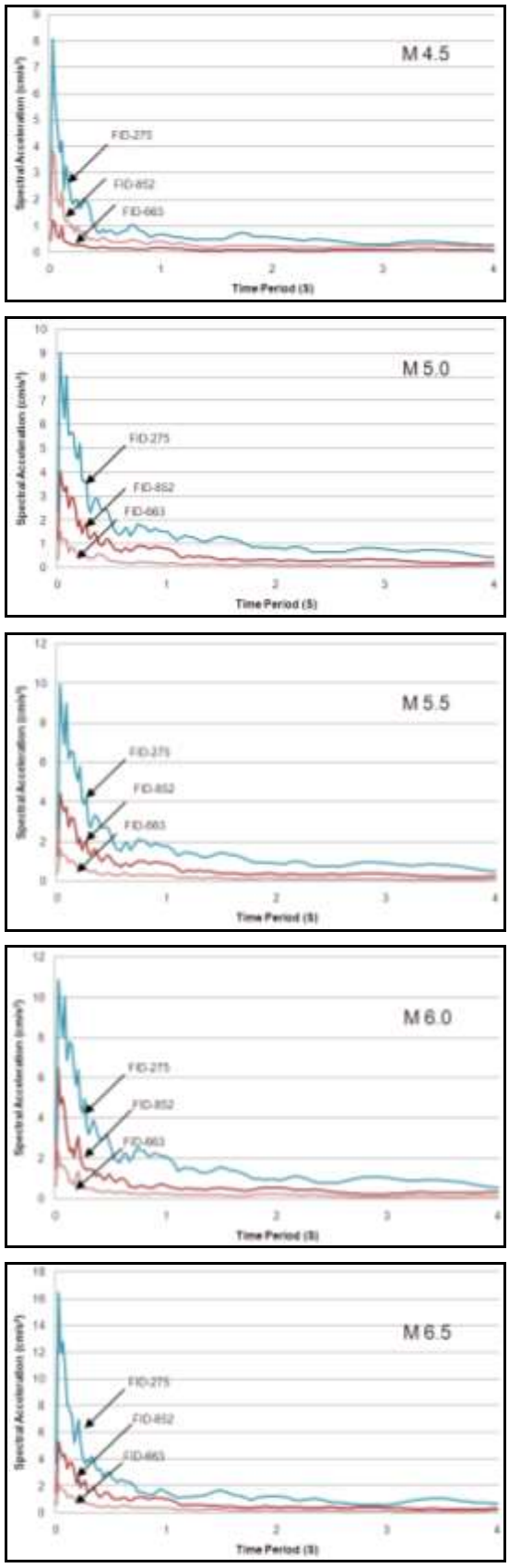

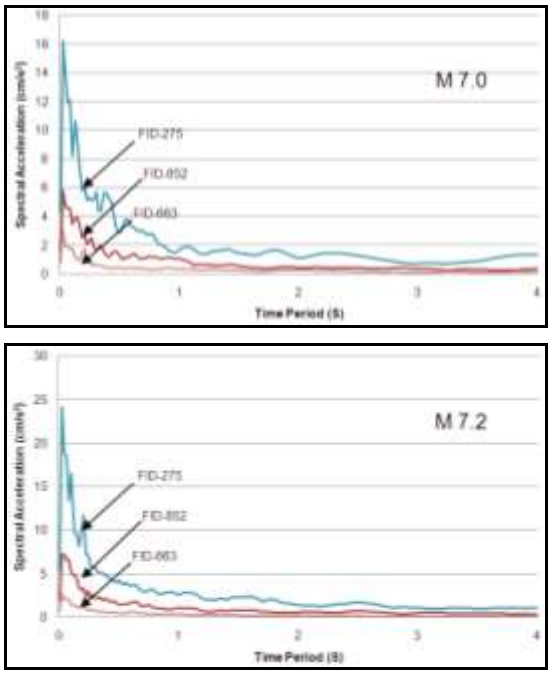

Fig 7 *Response spectra are generated from synthetic accelerograms for all three faults with respect to magnitude of the earthquake*

From the response spectra, it is observed that the spectral accelerations are increasing as the source of earthquake increases.

4. Conclusions

This study presents the generation of response spectrum using synthetic accelerograms at Rawatbhata power plant. For this purpose three active faults are considered and generated strong ground motions by using semi imperial approach. A MATLAB code is written to generate ground motion records due to the faults. It is observed that as the source of the earthquake increases, the amplitude of the ground motion, duration and energy content increases. Similarly, the spectral accelerations are also increases due to all three active faults.

References

1. Boore D.M., 1983, Stochastic simulation of high frequency ground motion based on seismological models of radiated Spectra. Bull Seism Soc Am., Vol.73, pp.1865–1894.
2. Brune, J. N., 1970, Tectonic stress and spectra of seismic shear waves from earthquakes, J. Geophys. Res., 1970, 75, 4997–5009.
3. Chenna Rajaram and Ramancharla Pradeep Kumar, 2014, Simulation of Ground Motion Characteristics of the 20 September 1999 Chi-Chi Earthquake Using Semi-Empirical Approach, Proc. of 15th Symposium on earthquake engineering, IIT-Roorkee, India.
4. Joshi A, Pushpa Kumari, Sandeep Singh, M. L. Sharma, 2012, Near-field and far-field simulation of accelerograms of Sikkim earthquake of September 18, 2011 using modified semi-empirical approach, Nat Hazards, Vol.64, pp.1034-1039
5. Joshi A, Midorikawa S, 2004, A simplified method for simulation of strong ground motion using rupture model of the earthquake source. Journal of Seismology, Vol.8, pp.467–484.
6. Joshi A, 2004, A simplified technique for simulating wide band strong ground motion for two recent Himalaya earthquakes. Pure Appl Geophys, Vol.161, pp.1777–1805.
7. Joshi A, Mohan K., 2008, Simulation of accelerograms from simplified deterministic approach for the 23rd October 2004 Niigata-ken Chuetsu earthquake, Journal of Seismology, Vol.12, pp.35–51.
8. Midorikawa S., 1993, Semi empirical estimation of peak ground acceleration from large earthquakes, Tectonophysics, Vol. 218, pp.287–295.
9. Steven L. Kramer., 1996, Geotechnical Earthquake Engineering, Pearson Publishers.
10. Bishnoi, L.R., 2014, Seismic Safety of Nuclear Power Plants, Proc. of 15th Symposium on earthquake engineering, IIT-Roorkee, India.
11. Sai Sumanth Reddy and Ramancharla Pradeep Kumar, 2011, Review of Nuclear Energy Demand in Urban Areas of India; vis-à-vis Seismic Disturbances, Proc. of Urban Safety Mega Cities in Asia, Mangolia.
12. Malhotra, S.K., 2010, Atomic Energy in India: A Historical Perspective, Nuclear India, Vol. 44, pp.7-19.